Desalination and Water Treatment
www.deswater.com
1944-3994/1944-3986 © 2012 Desalination Publications. All rights reserved
doi: 10/5004/dwt.2012.3259

Taylor & Francis
Taylor & Francis Group

45 (2012) 191–205
July

Dyes adsorption on low cost adsorbents: inorganic materials

Araceli Rodríguez*, Gabriel Ovejero, María Mestanza, Juan García*

Grupo de Catálisis y Procesos de Separación (CyPS), Departamento de Ingeniería Química, Facultad de Ciencias Químicas, Universidad Complutense de Madrid, Avda. Complutense s/n, 28040 Madrid, Spain
Tel. +34 91 394 4182/5207; Fax: +34 91 394 4114; emails: arodri@quim.ucm.es, juangcia@quim.ucm.es

Received 8 September 2011; Accepted 11 October 2011

ABSTRACT

A comparative study of liquid-phase adsorption of two dyes on several inorganic materials was carried out. The adsorbents used were bentonite, Fuller's earth, kaolinite, hydrotalcite and high-purity hydrotalcite Syntal HSA 696. The experimental results described the equilibrium adsorption capacity and were fitted to different isotherm equilibrium models. The effect of temperature, pH and surface modification were also studied. Bentonite, Fuller's earth and kaolinite presented higher adsorption capacity for methylene blue (MB), and hydrotalcite and Syntal HSA 696 were better for OII (orange II) adsorption.

Keywords: Adsorption; Clays; Methylene blue; Orange II; Wastewater; Dyes

1. Introduction

The discharge of dyes wastewaters into natural streams and rivers from the textile, paper, leather, and printing industries poses severe problems, as dyes impart toxicity to the aquatic life and they are also damaging to the aesthetic nature of the environment. Therefore it is important to search methods to treat them. Physical, chemical, and biological methods are available for the treatment of wastewaters discharged from these industries. In recent years, advanced oxidation processes (AOPs) have been intensively investigated. Homogeneous and heterogeneous Fenton reaction is already in use for industrial wastewater purification processes. However, many of the dyes used in these industries are stable to light and oxidation, as well as being resistant to aerobic/anaerobic digestion.

Adsorption has been found to present advantages in front of other techniques for treating wastewater: low-cost, simplicity, easy to perform and non-sensitive to toxic substances. On the environmental and economic side, the selection of the best adsorbent is a key issue that receives large attention. The solid should be cheap, susceptible to regeneration, inert, mechanically, chemically and thermally stable; besides it should present the adequate conformation (pellets, powder, granular) for the process in which it is going to be used. These are the reasons why the search of new adsorbents is carried out so vehemently. Many reviews have appeared lately in literature studying new adsorbents [1–4].

Methylene blue (MB), cationic dye, and orange II (OII), anionic dye, were selected as model compounds in order to evaluate the capacity of several materials for their removal from aqueous solutions in batch mode [5–7]. In this sense, the purpose of the present study was to investigate the effect of solution variables (temperature, pH) and surface solid modifications on the adsorption process of two dyes with different ionic character on five different inorganic materials including bentonite, kaolinite, Fuller's Earth, hydrotalcite and Syntal HSA 696.

*Corresponding authors.

The characterizations of the solids were also carried out. The equilibrium data of the adsorption processes were then evaluated to find a model that properly reproduced the experimental data.

2. Materials and methods

2.1. Materials

Five kinds of inorganic powder materials were used in this study: bentonite (supplied by TOLSA S.A.), kaolinite (Fluka), Fuller's Earth (Sigma-Aldrich), hydrotalcite (Sigma-Aldrich) and Syntal HSA 696 (Süd-Chemie). All the materials were used as received with no further purification.

2.2. Dye

The basic dye, MB was purchased from Alfa Aesar and the acidic dye, OII from Sigma-Aldrich. Both were used without further purification. The main characteristics of dyes used in this work and their structures are shown in Table 1. The solutions of dyes were prepared by dissolving accurately weighed amounts of MB and OII respectively in distilled water.

2.3. Analytical techniques

The dye was made up in solutions of concentration 300 mg l^{-1}, or 500 mg l^{-1} when needed. Calibration curve was prepared by recording the absorbance values for a range of known concentrations of MB solution at 631 nm. This wavelength (λ) was selected because the calibration was linear in a wider wavelength range than using λ_{max}. The OII solutions were measured at λ_{max} 482 nm. All measurements were made on a UV/Vis spectrophotometer (Shimadzu spectrophotometer UV-2401 PC).

2.4. Characterization of adsorbents

Textural characterization of clays was done by using N_2 adsorption-desorption at 77 K in a Micromeritics ASAP 2010 apparatus, and mercury intrusion porosimetry in a Thermo Finnigan Pascal 140–440. Scanning electron microscopy (SEM) was conducted at 15 kV using a JSM-6700F field emission scanning microscope and used to analyze the morphology of the solid samples; sample preparation involved dispersing them onto a carbon film supported by copper grids and sputtered with gold. Thermogravimetric analysis (TGA) experiments were performed with a heating rate of 10°C min^{-1} in inert atmosphere on a Seiko EXSTAR 6000 TGA Instrument, from 20°C to 900°C, at an helium flow rate of 30 ml min^{-1}. FTIR spectra were collected using a Nicolet Nexus-670 FTIR spectrophotometer at a resolution of 4 cm^{-1} in KBr tablets (2 mg of clay/98 mg KBr). X-ray Fluorescence (XRF) measurements were performed using a BRUKER S4 EXPLORER system, with software for data acquisition and analysis.

2.5. Adsorbents modifications

The solids were modified in order to improve their adsorption capacities, as it can be seen in Table 2. The references in which these treatments are deeply described are also included.

Table 1
Main characteristics of the dyes tested in this study

Dye	Structure	Chemical class	C.I. name	C.I. number	Molecular weight (g mol^{-1})	Molecular formulae	λ_{max} (nm)
Methylene blue (MB)	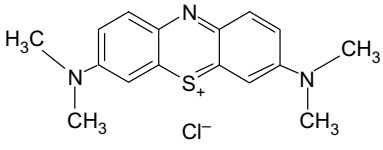	Cationic dye	Basic blue 9	52015	319.2	$C_{16}H_{18}ClN_3S$	631
Orange II (OII)	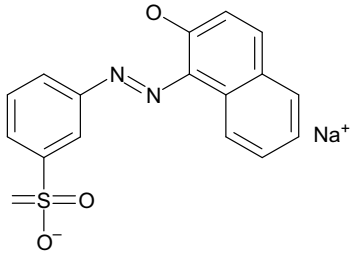	Anionic dye	Acid Orange A	15510	350.3	$C_{16}H_{11}N_2NaO_4S$	485

Table 2
Activation treatments tested

Material	Reference	Thermal treatments		Chemical treatments	
Bentonite	[18]	Calcination 450°C for 4, 5 h	Calcination 200°C for 2 h.	15 g of bentonite were mixed with 100 ml of H_2SO_4 5 M at 30°C for 4.5 h. Afterwards the solid sample was washed several times with ultrapure water	15 g of bentonite were mixed with 100 ml of NaOH 5 M at 30°C for 4.5 h. Afterwards the solid sample was washed several times with ultrapure water
Fuller's earth	[19]	Calcination 450°C for 4, 5 h	–	A portion of sample weighting 2.5 g was mixed with 250 ml of 6 M HCl at 95°C in a Pyrex flask with reflux for 24 h	A portion of sample weighting 2.5 g was mixed with 250 ml of 6 M NaOH at 95 °C in a Pyrex flask with reflux for 24 h
Kaolinite	[20]	Calcination 450°C for 4.5 h	–	Samples of 6 g of raw kaolinite were shaken with 100 ml of 1 M HNO_3 for 4 h in a Pyrex flask with reflux	Samples of 6 g of raw kaolinite were shaken with 100 ml of 1 M NaOH for 4 h in a Pyrex flask with reflux
Hydroalcite	–	–	–	–	–
Syntal HSA 696	[21]	Calcination 450°C for 4.5 h	–	–	–

Table 3
Experimental conditions in adsorption batch equilibrium experiments to study the influence of the pH

	pH	C_0 mg^{-1} l^{-1}	V ml^{-1}	W g^{-1}	T/°C
Bentonite	3-5-7-9	300	25	0.03	30
Fuller's earth	3-5-7-9	300	25	0.05	30
Syntal HSA 696	3-5-7-9	300	25	0.05	30
Syntal HSA 696 calcined	3-5-7-9	500	25	0.05	30

2.6. Adsorption experiments

Batch equilibrium experiments with the adsorbents were conducted using conical flasks immersed in a thermostatic bath. The samples were agitated to reach equilibrium. At the end of the contact time, a known volume of the solution was removed and centrifuged for the analysis of the supernatant.

The effect of pH on the adsorption of the dye on adsorbents was investigated by varying the initial pH solution from 3.0 to 9.0. The pH solution was adjusted with diluted solutions of strong acid (HCl) and/or strong base (NaOH) and recorded with a pH meter (Crison 2002). The experimental conditions for these experiments are described in Table 3.

3. Results and discussion

3.1. Characterization of adsorbents

Table 4 shows the results of N_2 and Hg porosimetries. The external surface (the corresponding to macro- and mesopores) was calculated applying the *t*-plot method to the experimental N_2 adsorption data. Fig. 1 shows the differential thermogravimetric analysis (DTG) curves obtained from the five solid samples under inert conditions.

Table 4
Results of the porosimetry analysis

	N_2 porosimetry		Hg porosimetry	
	S_{BET} m^2 g^{-1}	S_{ext} m^2 g^{-1}	ε %	ρ_{bulk} cm^3 g^{-1}
Bentonite	82.6	18.14	72.61	0.8464
Fuller's earth	77.5	63.9	82.81	0.4844
Kaolinite	7.1	4.4	79.78	0.6589
Hydrotalcite	13.4	13.4	–	–
Syntal HSA 696	12.0	12.0	69.69	0.4006
Syntal HSA 696 calcined	136.8	75.7	82.61	0.4379

All the solids possess good thermo stability in the range of temperature they were used (30–65°C). Hydrotalcite, Syntal HSA 696 and kaolinite presented lower humidity content than bentonite and Fuller's earth.

The results of XRF measurements are presented in Table 5. The analyses were carried out with the solids in the powder form, analysing them as if they were liquids. Hence the results included the humidity content of the material. Due to the technical characteristics of the analysis, the carbon could not be measured. As it was expected, the main elements presented in bentonite, Fuller's earth and kaolinite were oxygen and silicon. However, other species could be found in the solids, and

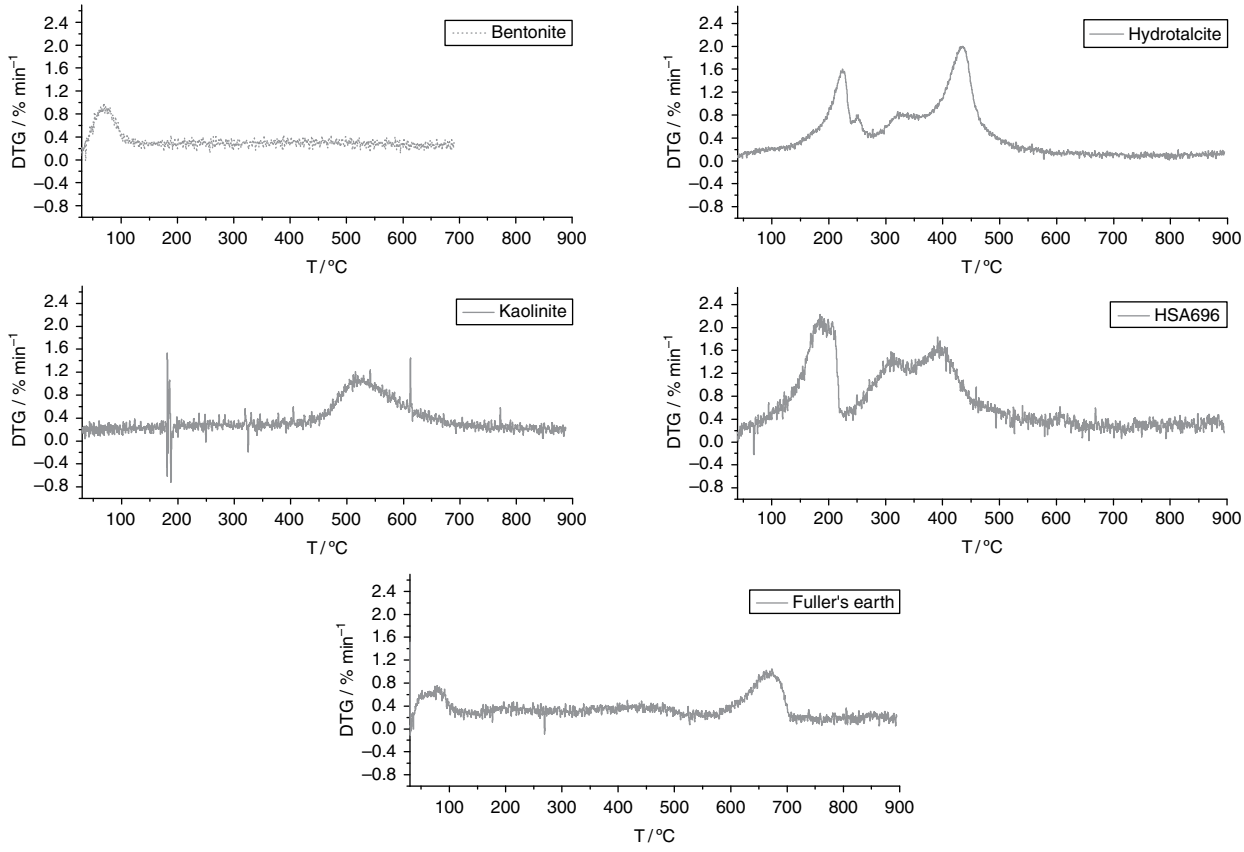

Fig. 1. DTA curves of the adsorbents at 10°C min^{-1} under 30 sccm helium flow rate.

Table 5
X-ray fluorescence results (%)

	Bentonite	Fuller's earth	Kaolinite	Hydrotalcite	Syntal HSA 696
Al	2.71	5.6	19.96	31.72	25.28
Ba	–	–	0.07	–	–
Ca	0.19	7.05	0.05	0.02	0.7
Cu	–	–	0.04	–	–
Fe	1.45	3.2	0.46	–	–
K	0.9	0.75	1.71	–	–
Mg	15.1	5.63	–	24.04	30.33
Mn	0.07	0.07	–	–	–
Na	0.83	–	–	–	–
O	48.21	47.41	49.69	44.14	44.24
P	0.01	0.4	0.27	0.01	0.11
Pb	–	–	0.41	–	–
Rb	0.01	0.01	0.01	–	–
S	–	0.04	–	–	–
Si	30.28	29.44	27.02	0.07	0.32
Sr	0.01	0.02	0.04	–	–
Ti	–	0.35	0.27	–	–
Zn	0.01	0.01	–	0.01	0.01
Zr	0.01	0.02	–	–	–

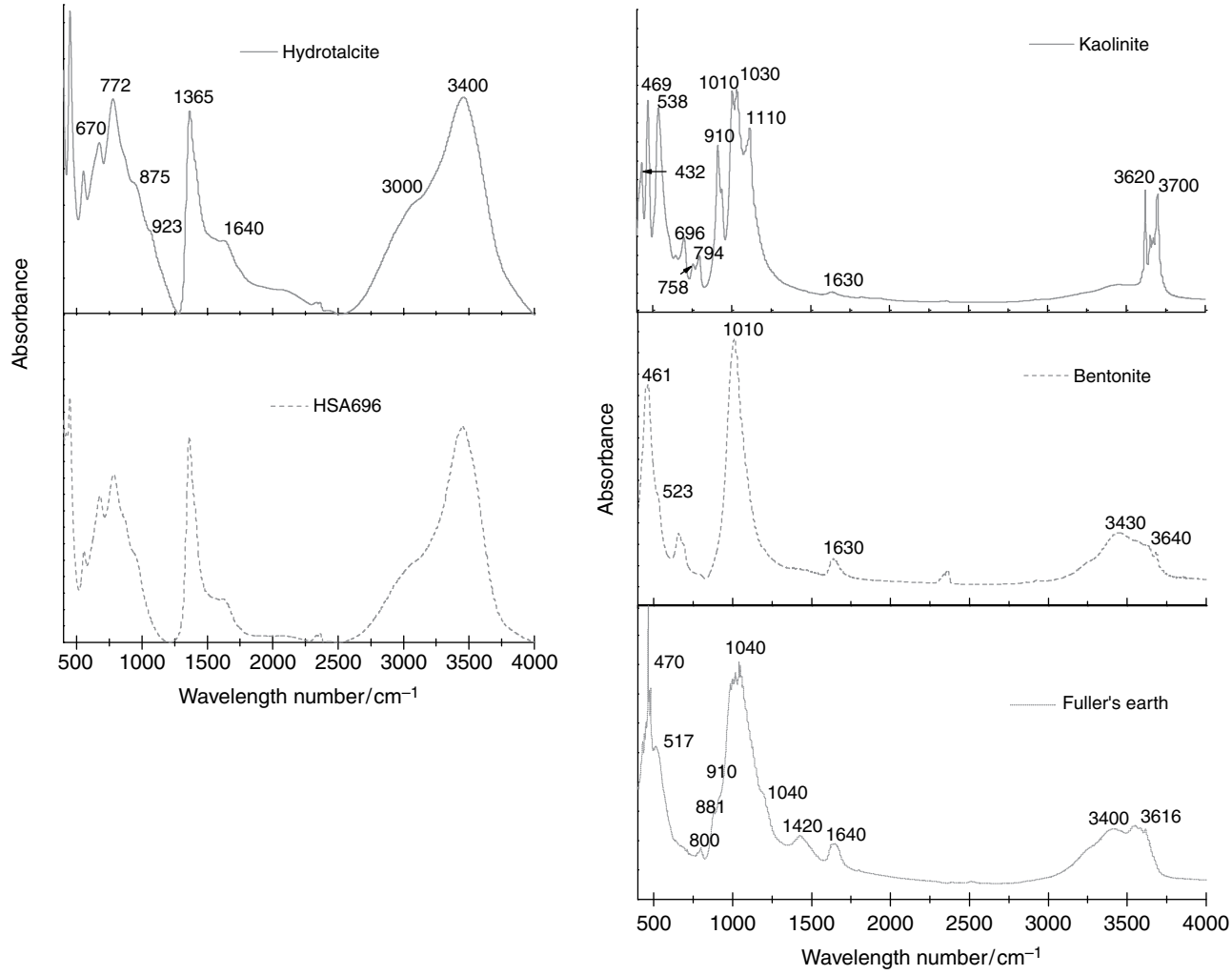

Fig. 2. FTIR of the adsorbents.

they were Al for kaolinite; Mg, Al and Fe for bentonite; and Ca, Mg, Al and Fe for Fuller's earth. However hydrotalcite and Syntal HSA 696 were high purity mixed oxides of Mg and Al. The content of Al in hydrotalcite is higher than the content in Syntal HSA 696.

The FTIR spectrums of the five solids are presented in Fig. 2. They were divided in two groups due to their similarities: bentonite, Fuller's earth and kaolinite in a group (cationic clays), and hydrotalcite and Syntal HSA 696 in another (anionic clays). The main peaks in every spectrum had been identified and described in the Table 6.

The SEM images of the five solids are shown (Fig. 3), just to show that most of the particles used were of similar sizes. In Fuller's earth image it could be seen two types of materials, probably montmorillonite and paligorskite [8]. Kaolinite is composed by different sizes planar sheets. Both hydrotalcite and Syntal HSA 696 presented very similar appearance.

3.2. Adsorption experiments

The equilibrium time between the adsorbate in liquid phase and the adsorbed on the solid is reached with a rate which depends not only on the diffusion of the components in the adsorbent but also on the adsorbent/adsorbate interaction. Therefore the adsorption experiments were as long as necessary to reach a constant dye liquid-phase concentration (equilibrium times longer than 2 h in all the systems adsorbent-adsorbate).

3.2.1. Effect of surface modifications and of the pH of the solution

Surface modification is a key step concerning the application of clays in adsorption. The solids were modified in order to improve their adsorption capacities. It has been stated that the structural changes of bentonite, Fuller´s earth, Kaolinite and Syntal HSA 696 with thermal treatment affect the specific surface area and

Table 6
FTIR peaks identification

Material	Wavelength number/cm^{-1}	Assignement
Bentonite [22]	3640	Al-Mg-OH stretching
	3430	H-O-H stretching (for H2O)
	1630	H-O-H bending
	1010	Si-O stretching
	523	Al-Si-O bending
	461	Si-O-Si bending
Kaolinite [23,24]	3694-3620	O-H stretching band (Typical of kaolin gruoup)
	1630	Presence of water
	1110	Quartz
	1033-1005	Si-O
	910	Al_2OH deformation (internal surface OH)
	794-757	Si-O-Si
	695	Si-O-Si
	538	Al-O-Si
	469-432	SiO_2
Fuller's earth [25,26]	3616	Al_2OH groups (Typical of paligorskite)
	3400	H-O-H stretching
	1635	H-O-H bending
	1425	Calcite impurity
	1040 band	Silica amorphous
	910	Al-Al-OH deformation
	881	Al-Fe-OH deformation
	800	Three dimensional amorphous silica phase
	517	Si-O-Al (octahedral) bending vibrations
	470	Si-O-Si bending vibration
Hydrotalcite and Syntal HSA 696 [27]	3400 band	Interlaminar water
	1640	H-O-H deformation
	1360, 875, 670	Carbonate ions
	1090-922-772	Al-OH bonds

adsorption capacity of these clays. On the other hand, the chemical treatments (Table 2), affect the adsorption capacity in several aspects. In the next paragraph, we show these effects on adsorption capacity. The references in which these treatments are deeply described are in Table 2.

Also, the pH of the solution had a significant effect on the adsorption capacity reached in most of the systems adsorbate-adsorbent. The results of each pair dye-adsorbent are described next:

- Bentonite: the results in Fig. 4a show that MB could be adsorbed on bentonite. Adsorbent modifications did not increase the adsorption capacity, but the thermal ones did not modify the capacity, which can be useful if a thermal regeneration of the bentonite was searched. However, the chemical treatments decreased the affinity of bentonite towards the MB, specially the acid one, which reduced the adsorption capacity, compared with the raw ones, more than a 90%. As the maximum capacities were reached for the raw solid, this was the adsorbent selected to continue the study. Consequently, it was important to focus on the tendency of adsorption capacity with pH and, as it can be seen in Fig. 4a, the pH analyzed that maximizes q_e was pH = 7. Bagane and Guiza in 2000 [9] stated that the capacity of adsorption reached a maximum at pH = 7 due to the compromise value got at this pH between the Columbians and the van der Waals forces. However, the bentonite did not adsorb at all OII, neither raw nor activated (Fig. 4b).
- Fuller's earth. Using MB as adsorbate (Fig. 5a), the raw sample and the activated ones by means of basic

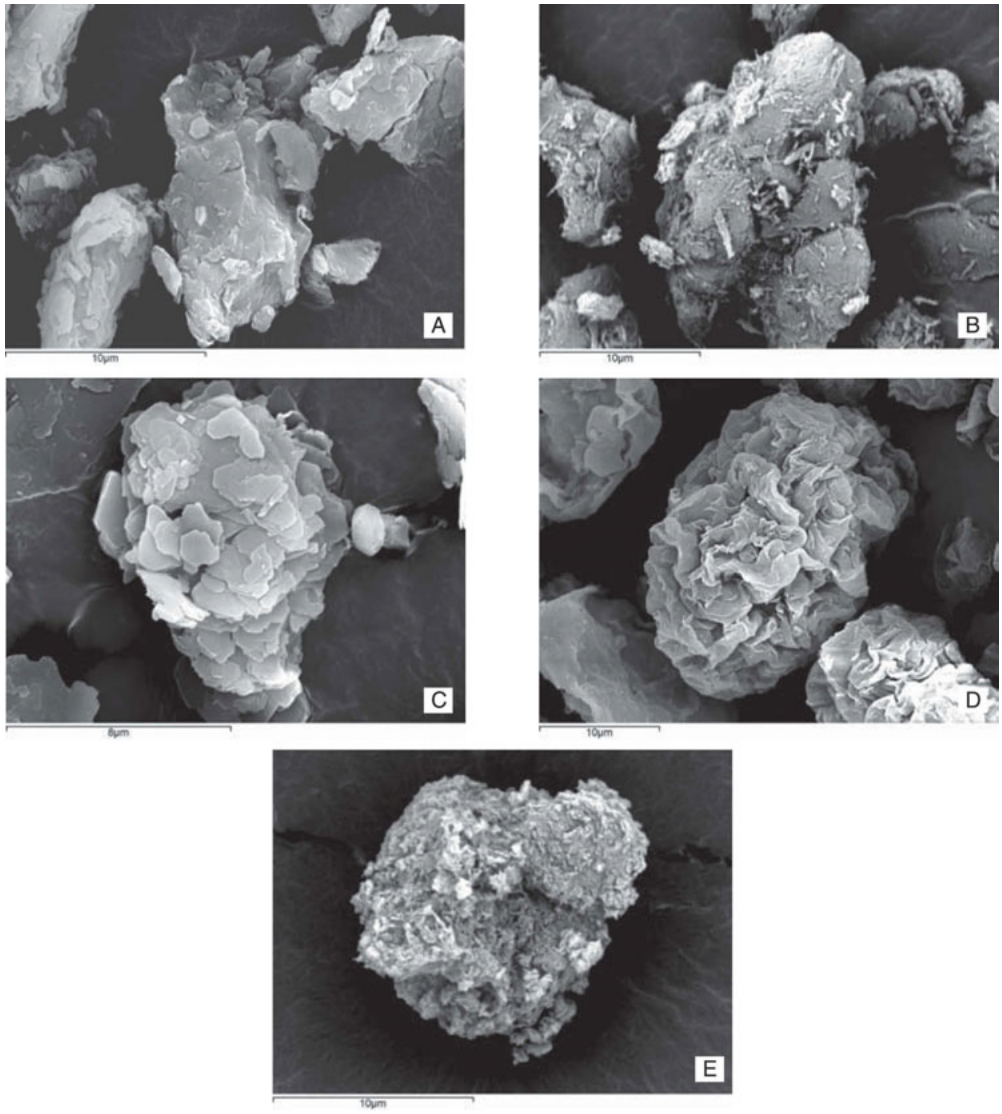

Fig. 3. SEM micrograph showing general appearance of the adsorbents: (a) Bentonite, (b) Fuller's earth, (c) Kaolinite, (d) Hydrotalcite, (e) Syntal HSA 696.

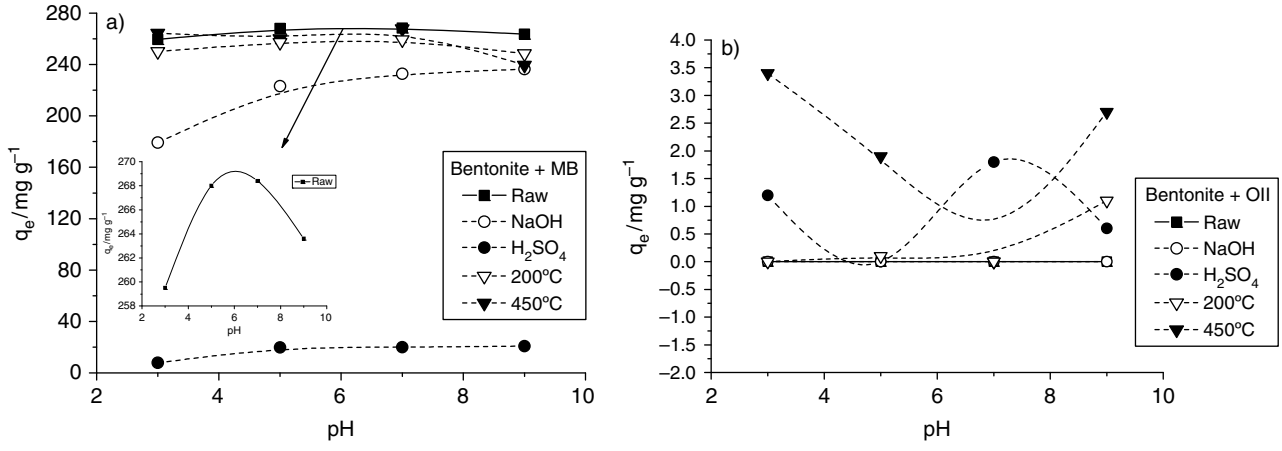

Fig. 4. Effect of pH on adsorption capacity on Bentonite: (a) MB and (b) OII.

chemical as well as thermal treatments showed almost the same capacity, and the acid activated suffered a decrease in its capacity of 100%. The activation treatments did not significantly increase the capacity and the raw material at pH = 5 was selected to continue the study. If the adsorbate considered is the OII (Fig. 5b), it can be seen that, as occurred with MB, the acid treated sample did not adsorb it at all. But in this case, the basic treated sample showed the maximum adsorption capacity at pH = 3, reaching a value of $q_e \approx$ 30 mg g^{-1}, versus the $q_e \approx 12$ mg g^{-1} obtained with the non treated clay. Hence, if the effluent contained both dyes, it may be useful to modify Fuller's earth with NaOH to get both adsorbed, despite of the reduction of the affinity of this solid towards MB.

- Kaolinite. The results of the adsorption of MB on kaolinite are shown in Fig. 6a. The maximum capacity is reached for the raw kaolinite and pH = 3, and took a value of almost 18 mg g^{-1}. The adsorption of OII on kaolinite was assayed but the results indicated that it was adsorbed at all, neither on the raw clay nor in the activated ones. As the equilibrium capacity is quite low compared with the ones obtained for bentonite and Fuller's earth, the study of the systems dye-kaolinite continued no longer.
- Hydrotalcite. Fig. 6b shows that this sample did not adsorb MB but did OII, with a maximum capacity at pH = 3 of almost 30 mg g^{-1}. The study of the systems dye-hydrotalcite did not continued due to the low capacities showed in these experiences.
- Syntal HSA 696. The results are shown in Figs. 7a and 7b. In both figures it can be seen that the adsorption capacities of the dyes were enhanced after calcination. The affinity of this solid is higher for OII than for MB, as it was expected due to the behaviour of the hydrotalcite, which essentially is the same material than Syntal HSA 696.

The results obtained in this work were compared with values found in literature. It can be seen in Table 7

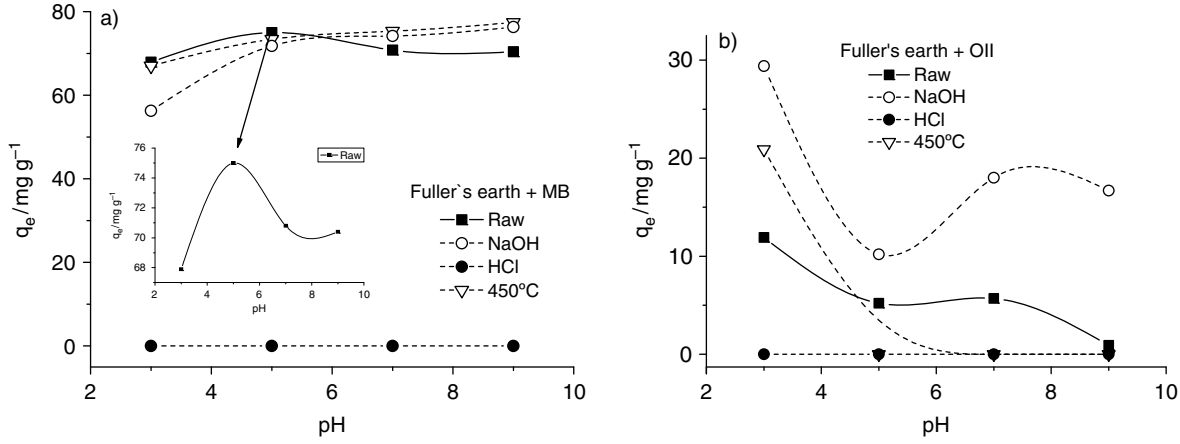

Fig. 5. Effect of pH on adsorption capacity on Fuller's earth: (a) MB and (b) OII.

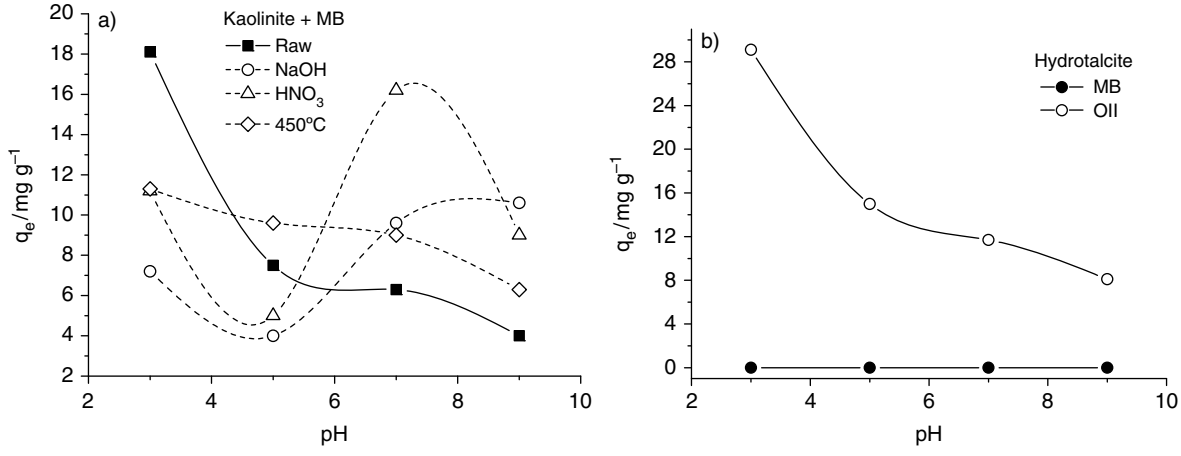

Fig. 6. Effect of pH on adsorption capacity: (a) Kaolinite-MB and (b) Hydrotalcite.

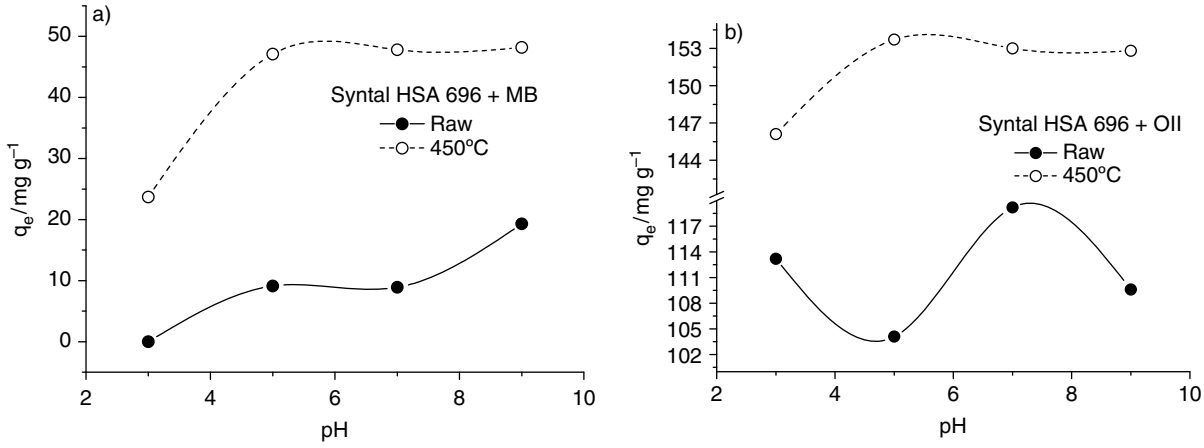

Fig. 7. Effect of pH on adsorption capacity on Syntal HSA 696: (a) MB and (b) OII.

Table 7
Adsorption capacities of MB on different solids

Reference	Adsorbate: Methylene blue	
	Adsorbent	Adsorption capacity mg g^{-1}
[28]	Montmorillonite	830
[5]	Bamboo based activated carbon	454
[12]	F-400 (commercial activated carbon)	425
[29]	Composite of chitosan and activated clay	340
This study	Bentonite	315
[30]	Diatomaceous silica	110
[11]	Sepiolite	80
[11]	Pansil	70
This study	Fuller's earth	70
[31]	Clay	60
[32]	Zeolite MCM-22	57.5
[33]	Carbon nanofibres	55
[33]	Carbon nanotubes	45
[10]	Perlite	6.4
	Adsorbate: Orange II	
	Adsorbent	Adsorption capacity mg g^{-1}
Present study	Syntal HSA 696 calcined	900
[34]	Titania aerogel	400
[35]	Commercial activated carbon	400
[33]	F-400 (commercial activated carbon)	380
[35]	Sludge adsorbent	180
[35]	Activated carbon fiber	150
Present study	Syntal HSA 696	120
[33]	Carbon nanofibres	80
[33]	Carbon nanotubes	70

that carbonaceous materials presented good affinity towards the cationic dye, besides, cationic clays presented good results. The carbonaceous materials also adsorbed large amounts the anionic dye (OII); and the anionic clays referred also retained this compound. Activated carbon is a good option to remove, either anionic or cationic dyes from wastewater. However, clays usually are cheaper than activated carbon, so bentonite or sepiolite might be used as adsorbents to remove cationic dyes.

3.2.2. Effect of temperature on adsorption capacity

In this work several systems adsorbate-adsorbent were studied. One of the most important information of an adsorption system is the isotherm equilibrium data, which relate equilibrium capacity q_e, understood as the adsorbate concentration in the solid phase, with the equilibrium concentration in liquid phase, C_e. These data may be obtained at a constant temperature. Temperature had a very important effect on adsorption. Usually, and above all, in gas phase, adsorption is exothermic; it means that the adsorption capacity decreases with increasing temperatures. However, in liquid phase, the contrary tendency may be found. Increasing the temperature is known to increase the rate of diffusion of the adsorbate molecules across the external boundary layer and in the internal pores of the adsorbent particle, due to the decrease in the viscosity of the solution. In addition, changing the temperature will change the equilibrium capacity of the adsorbent for a particular adsorbate [10]. Besides, as we demonstrated above, the pH of the solution had a significantly influence in the sorption capacity. The experimental conditions used to obtain the experimental data are listed in Table 8.

Figs. 8a and 8b show the results of adsorption capacity experiments carried out using MB as adsorbate, and bentonite and Fuller's earth as adsorbents at different temperatures (30°C, 40°C and 65°C). As it can be seen, temperature in the range assayed had no effect on the adsorption capacity on bentonite. Bagane and Guiza in 2000 [9] suggested that this phenomenon is due to no change in the structure of the clay was observed between 5°C and 30°C, not was the stability of the colorant. Looking at the DTG curves, it can be stated that no significant changes in the structure of the bentonite occurred heating from 30°C to 65°C (*see* Fig. 1). However, we propose that these insignificant changes in the adsorption capacity of MB on bentonite are related to the low values of heat interchanged during the sorption process.

Nevertheless, when the adsorbent used is Fuller's earth, the influence of temperature in adsorption capacity was clear: increasing temperatures led to increasing capacities. This was also observed in literature for the

Table 8
Experimental conditions in adsorption batch equilibrium experiments to obtain the isotherm experimental data

	Adsorbate	pH	C_0 mg^{-1} l^{-1}	V ml^{-1}	W g^{-1}	T/°C
Bentonite	MB	7	500	25	0.006–0.056	30. 40. 65
Fuller's earth	MB	5	300	25	0.020–0.135	30. 40. 65
Syntal HSA 696	OII	7	300	25	0.01–0.12	30. 65
Syntal HSA 696 calcined	OII	7	500	25	0.0002–0.002	30. 65

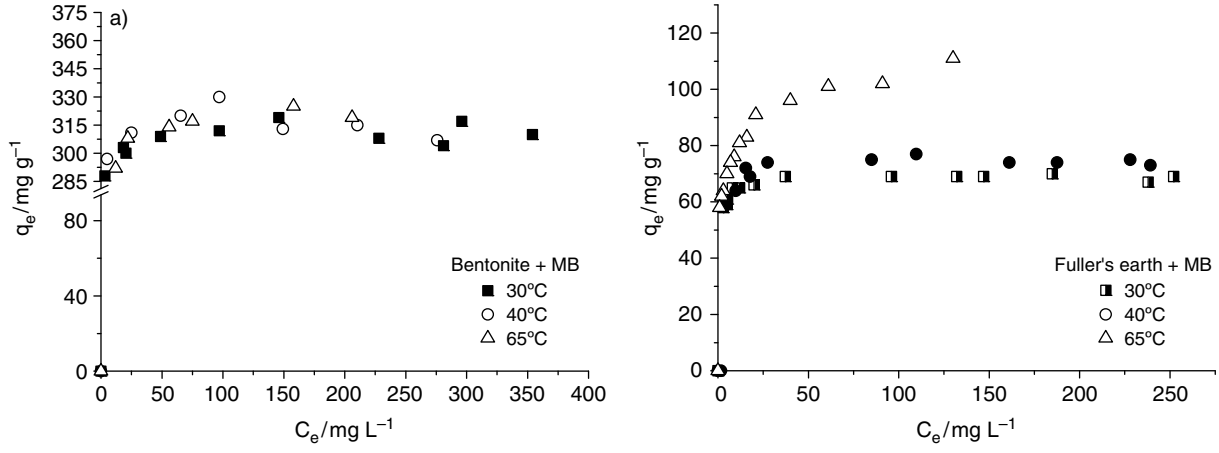

Fig. 8. Adsortion capacity at different temperatures: (a) Bentonite-MB and (b) Fuller's earth-MB.

same system [10] and for systems MB-clays [11] and MB-carbonaceous materials [12].

The MB adsorption capacity of bentonite is three times higher than the presented by Fuller's earth, with maximum values of capacity at 30°C of 315 mg g^{-1} for the former versus 70 mg g^{-1} for the later. These values were similar to the ones found in literature for the same adsorbate MB [13].

The experimental isotherms obtained for both systems might be classified according to Giles classification [14] as type H-2. This is a special case of the L curve, in which the affinity of the solute towards the solid is so high that in dilute solutions (or with high loads of adsorbents) it is completely adsorbed, or at least there is no measurable amount remaining in the solution. Therefore, the initial part of the isotherm is vertical. Beyond, the inflection, the curve followed a common L form.

Figs. 9a and 9b show the results of the systems Syntal HSA 696-OII, raw and calcined respectively. At naked eye, it might be assured that the thermal treatment led to a significant adsorption capacity increase that might be due to the change in the Syntal HSA 696 structure. Crystalline degree decreased with calcination according to the observations in X-ray diffractograms of the clays. However the main structure of the material was not destroyed. Besides, the N_2 adsorption data at 77 K indicated that the porosity of the solid was developed after calcinations, it specific surface increased almost tenfold, what might explain the increase in adsorption capacity. Even more, the tendency of the adsorption capacity of OII on Syntal HSA 696 depends on the previous treatment of the solid. If the Syntal HSA 696 is used as received, q_e decreased with increasing temperatures (exothermic), but if it was previously calcined, q_e increased with rising temperatures (endothermic), as occurred in the system Fuller's earth-MB. This led to the conclusion that the behaviour of the isotherm experimental data did not only depend on the adsorbate but also on the adsorbent. Therefore, the greatest adsorption capacities were obtained for the calcined Syntal HSA 696 using OII as adsorbate.

3.2.3. Adsorption isotherms modelling

From a design point of view it was necessary to find models fit experimental data. In adsorption, empirical or theoretical models either may be found. These models represent the relationship between the amount of solute adsorbed per unit of adsorbent mass once the equilibrium is reached (q_e) and the concentration of solute in solution (C_e). The most common models used in liquid phase adsorption are Freundlich and Langmuir equations. However in this study, not only those models were used but also Sips and Redlich–Peterson (R-P) equations [15].

Langmuir isotherm:

$$q_e = \frac{q_{sat} b C e}{1 + b C_e} \quad (1)$$

where q_{sat} (mg.g^{-1}) and b (l. mg^{-1}) are Langmuir constants, which are indicators of the maximum adsorption capacity and the affinity of the binding sites, respectively.

Freundlich isotherm:

$$q_e = K_F C_e^{1/n} \quad (2)$$

where K_F (mg.g^{-1}) and n (dimensionless) are the Freundlich constants, indicating adsorption capacity and adsorption intensity, respectively.

Sips equation (Langmuir–Freundlich):

Recognising the problem of the unlimited increase in the adsorbed amount with an increase in concentration in Freundlich's equation, Sips proposed an equation with a finite limit when the concentration is sufficiently high:

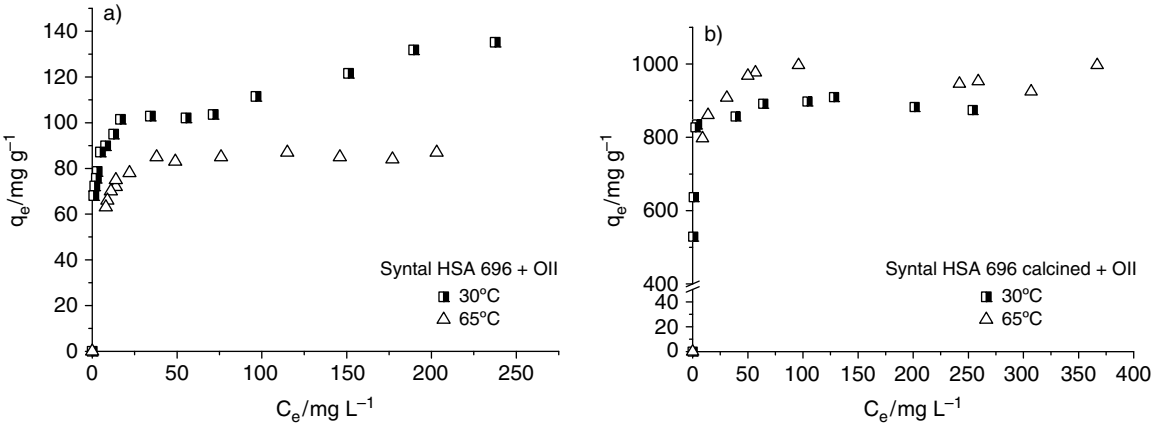

Fig. 9. Adsortion capacity at different temperatures: (a) Syntal HSA 696-OII and (b) Syntal HSA 696 calcined-OII.

$$q_e = q_{sat}\frac{(bC_e)^{1/n}}{1+(bC_e)^{1/n}} \quad (3)$$

where q_{sat} (mg g^{-1}) is the saturation capacity, and can be either taken as a constant or temperature dependent, b (l mg^{-1}) is the affinity constant, n (–) is the parameter characterising the system heterogeneity. If n = 1. Langmuir equation would be recovered.

Redlich-Peterson:

The R-P isotherm is more versatile than the Langmuir and Freundlich isotherms, because can be applied either in homogeneous or heterogeneous systems. R-P equation is represented by Eq. (4) where k_R (l g^{-1}) and a_R (l mg^{-1}) are the parameters of the model, and β is an exponent which changes between 0 and 1. This isotherm combines elements from both the Langmuir and Freundlich equations, and the mechanism of adsorption is a hybrid and does not follow ideal monolayer adsorption. The isotherm has a linear dependence on concentration in the numerator and an exponential function in the denominator:

$$q_e = \frac{k_R C_e}{1+a_R C_e^{\beta}} \quad (4)$$

The results of these fittings are shown in Table 9. It can be seen that the highest correlations coefficients were the corresponding to Sips and R-P as it was expected because these models have three adjusting parameters instead of two, as Langmuir and Freundlich models. However it was important to determine if this better fitting deserved the more complicate calculus. For this reason two more error indicators were calculated. One of them is the standard deviation (S.D. %). calculated using the following equation:

Table 9
Adsorption isotherms model parameters

Pair dye-adsorbent		T °C	Langmuir			Freundlich		
			q_{sat} mg g^{-1}	b l mg^{-1}	r^2	K_f l g^{-1}	n	r^2
Methylene blue	Bentonite	30	303	27.6	0.967	265.5	32.8	0.9857
		40	308	23	0.9762	268.5	28.9	0.9852
		65	309.2	5.4	0.982	255.8	23.5	0.9806
	Fuller's earth	30	69.1	1.5	0.9964	58.4	30.9	0.989
		40	77.6	0.45	0.9765	46.7	9.9	0.8519
		65	100.1	0.57	0.9404	55.7	7	0.9946
Orange II	Syntal HSA 696	30	110.4	1.05	0.9168	10.16	9.22	0.9807
		65	88.32	0.34	0.9959	58.3	12.37	0.9766
	Syntal HSA 696 calcined	30	893.8	2.9	0.9942	685	18	0.9386
		65	979.3	0.52	0.9915	795.06	27.4	0.787

Pair dye-adsorbent		T °C	Sips				Redlich-Peterson			
			q_{sat} mg g^{-1}	b l mg^{-1}	n	r^2	k_R l g^{-1}	a_R l mg^{-1}	β	r^2
Methylene blue	Bentonite	30	323.7	199.8	3.31	0.9946	21651	78.7	0.98	0.9901
		40	330.1	122.3	3.1	0.9935	14927.6	53	0.97	0.9907
		65	325.1	18.2	2.3	0.9904	2834	10.06	0.98	0.9877
	Fuller's earth	30	69.4	2	1.2	0.9966	109.2	1.6	0.99	0.9964
		40	74.63	0.41	0.61	0.9934	26.3	0.27	1.05	0.9866
		65	185.6	0.03	3.75	0.9965	387.9	6.5	0.87	0.9959
Orange II	Syntal HSA 696	30	119.3	1.71	2.26	0.9935	1122.2	15.4	0.9	0.9813
		65	86.7	0.26	0.75	0.9971	23.65	0.23	1.02	0.9971
	Syntal HSA 696 calcined	30	889.2	2.64	0.87	0.995	2305.8	2.48	1.01	0.9951
		65	968	0.31	0.68	0.9927	340.6	0.3	1.02	0.9937

$$\text{S.D.}(\%) = \sqrt{\frac{\sum_{i=1}^{n}\left[\left(q_{exp} - q_{cal}\right)/q_{exp}\right]^2}{n-1}}100 \quad (5)$$

where the subscripts *exp* and *cal* refer to the experimental and the calculated data, and n is the number of data points [16]. With the aim to compare models with different number of parameters, the hybrid error function (HYBRID) was studied:

$$\text{HYBRID}(\%) = \frac{100}{n-p}\sum_{i=1}^{n}\left[\frac{\left(q_{exp} - q_{cal}\right)^2}{q_{exp}}\right] \quad (6)$$

where n is the number of data points and p the number of parameters within the equation, S.D. takes into account the number of experimental data points. However, HYBRID is already considering, not only the number of experimental data points, but also the model. The values are listed in Table 10.

From the results in Table 10 several conclusions can be deduced. For the system MB-bentonite, despite of the correlation coefficients obtained for Sips and R-P were very similar, the values of S.D. and HYBRID for Sips were quite lower than the ones for R-P model. However, for the system MB-Fuller's Earth, Langmuir and Sips equations could be comparable. In the adsorption system OII-Syntal HSA 696, Sips was the model that better fitted the experimental data, but if the adsorbent was previously calcined, all the models tested, but Freundlich, could be properly used to reproduce the experimental data. It is important to remark that, despite of the larger degree of complexity of Sips model, the advantage was clear: it reproduced much better the adsorption systems assayed. However, if the Sips model is going to be used, is recommendable to fit in advance the experimental data to Langmuir and Freundlich with the aim to calculate previous values of q_{sat}, b and n. These values could be used as initial values for the parameters of Sips equation, because the non-linear fitting is easier for those models due to they only have two adjusting parameters instead of the three presented by Sips.

3.2.4. Adsorption thermodynamics

To calculate the thermodynamic parameters, Sips equation was used due to it provided the best experimental data fit. Q in the Langmuir equation is the isosteric heat, invariant with the surface loading, but in the Sips equation the parameter Q is only the measure of the adsorption heat and can be calculated from the dependence of b (affinity constant) with temperature:

$$b = b_\infty \exp\left(\frac{Q}{RT}\right) \quad (7)$$

The parameter Q defined in the affinity constant b is the isosteric heat at the fractional loading of 0.5 [17]. Plotting, ln (b) versus $1/T$ the slope correspond to Q/R.

Table 10
Calculated errors comparing experimental data and isotherm models predictions

		Methylene blue						Orange II			
		Bentonite			Fuller's Earth			Syntal HSA 696		Syntal HSA 696 calcined	
		30°C	40°C	65°C	30°C	40°C	65°C	30°C	65°C	30°C	65°C
Langmuir	r^2	0.9670	0.9762	0.9820	0.9964	0.9765	0.9404	0.9168	0.9959	0.9942	0.9915
	SD (%)	5.7	5.2	4.6	1.8	14.1	9.4	7.8	1.9	2.6	2.7
	HYBRID (%)	92.4	87.7	69	2.4	128.3	69	56.7	3.1	59	80
Freundlich	r^2	0.9857	0.9852	0.9806	0.9890	0.8519	0.9946	0.9807	0.9766	0.9386	0.9787
	SD (%)	3.5	4.1	3.6	3.3	10.2	2.4	3.9	4.8	10.2	4.6
	HYBRID (%)	37.5	56.7	41.1	7.9	78.6	5.5	16.1	18.5	748.2	210
Sips	r^2	0.9946	0.9935	0.9904	0.9966	0.9934	0.9965	0.9935	0.9971	0.9950	0.9927
	SD (%)	2.1	2.6	2.4	1.9	17.6	2	3.5	1.6	2.6	2.6
	HYBRID (%)	15.4	26.7	21.1	2.7	221.9	4.1	16.2	2.4	60.6	80.7
Redlich-Peterson	r^2	0.9901	0.9907	0.9877	0.9964	0.9866	0.9959	0.9813	0.9971	0.9951	0.9937
	SD (%)	3.2	4.1	3.2	3.6	15.7	2.3	3.6	4.6	2.5	4.3
	HYBRID (%)	34.7	65.3	40.7	10.8	176.4	5.5	15.2	20.9	58	215.3

Table 11
Calculated Q (kJ.mol^{-1}) for the four systems tested

		Q kJ^{-1} mol^{-1}
MB	Bentonite	59.8
	Fuller's Earth	100.6
OII	Syntal HSA 696	45.9
	Syntal HSA 696 calcined	52.2

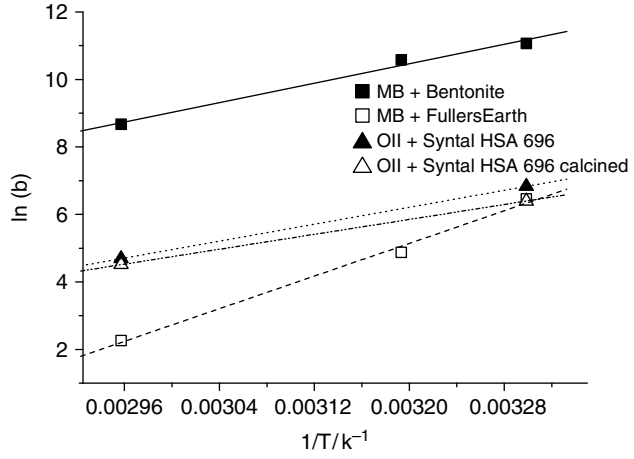

Fig. 10. Isosteric heats of adsorption.

The values of Q (KJ.mol^{-1}) are listed in Table 11. The plots are presented in Fig. 10.

From Fig. 10, the isosteric heats were calculated. As it was expected, Q in MB-bentonite system was lower than Q in MB-Fuller's Earth, indicating that the effect of temperature in adsorption capacity would be sharper in the latest system.

4. Conclusions

Following conclusions can be drawn from the present study of adsorption of MB and OII (cationic and anionic dye respectively) on several adsorbents. First of all, and as it was expected, the cationic clays mainly adsorbed the cationic dye (MB) and the anionic clays did adsorb the anionic one (OII). The different chemical surface treatment did not significantly enhance the adsorption capacity, but Fuller's Earth capacity for the OII increased when it was subjected to a treatment with NaOH. Besides the capacity of Syntal HSA 696 increased significantly when it was calcined at 450°C. The experimental adsorption capacities measured varied in the next way:

- MB: bentonite > Fuller's Earth > Syntal HSA 696 calcined > kaolinite > Syntal HSA 696 raw > hydrotalcite.
- OII: Syntal HSA calcined > Syntal HSA 696 raw > Hydrotalcite > Fuller's Earth + NaOH > kaolinite = bentonite (≈ 0 mg g^{-1}).

The adsorption capacity depended not only on the adsorbate but also on the adsorbent. In the system MB-bentonite any influence of the temperature was observed. However in the system MB-Fuller's Earth, the adsorption process was endothermic: increasing temperatures led to higher adsorption capacities. In the case of the OII, when the Syntal HSA 696 was used as received the adsorption of the dye was exothermic (increasing temperatures meant decreasing capacities), but if the solid was previously calcined at 450°C, the adsorption resulted in an endothermic process.

All the experimental data were fitted to the different adsorption equilibrium isotherm models, such as Freundlich, Langmuir, Sips and Redlich-Peterson. The study of the errors indicated that the model that best reproduced the experimental data measured was Sips in every system dye-solid.

Acknowledgements

The authors gratefully acknowledge the financial support from Ministerio de Educación y Ciencia by CONSOLIDER Program through TRAGUA Network CSD2006-44. CTQ2008-02728. Ph D Grants (FPU AP2007-01198) and Comunidad de Madrid through REMTAVARES Network *S2009/AMB-1588*.

References

[1] G. Crini, Non-conventional low-cost adsorbents for dye removal: A review, Bioresour. Technol., 97 (2006) 1061–85.
[2] Q.U. Jiuhui, Research progress of novel adsorption processes in water purification: A review, J. Environ. Sci., 20 (2008) 1–13.
[3] V.K. Gupta, Application of low-cost adsorbents for dye removal: A review, J. Environ. Manage., 90 (8) (2009) 2313–2342.
[4] S. Karcher, A. Kornmüller and M. Jekel, Screening of commercial sorbents for the removal of reactive dyes, Dyes Pigments, 51 (2001) 111–125.
[5] B.H. Hameed, A.T.M. Din and A.L. Ahmad, Adsorption of methylene blue on bamboo-based activated carbon: Kinetics and equilibrium studies, J. Hazard. Mater., 141 (2007) 819–825.
[6] B.H. Hameed, A.L. Ahmad and K.N.A. Latif, Adsorption of basic dye on activated carbon prepared from rattan sawdust, Dyes Pigm., 75 (2007) 143–149.
[7] D. Kavitha and C. Namasivayam, Experimental and kinetic studies on methylene blue adsorption by coir pith carbon, Bioresour. Technol., 98 (2007) 14–21.
[8] G. Ovejero, M.D. Romero, I. Diaz, M. Mestanza and E. Diez, Bentonite as an alternative adsorbent for the purification of styrene monomer: Adsorption kinetics, equilibrium and process design, adsorption kinetics, equilibrium and process design, Adsorpt. Sci. Technol., 28 (2010) 101–123.
[9] M. Bagane and S. Guiza, Elimination d'un colorant des effluents de l'industrie textile par adsorption, Ann. Chim. Sci. Mat., 25 (2000) 615–626.
[10] M. Doğan, Y. Özdemir and M. Alkan, Adsorption kinetics and mechanism of cationic methyl violet and methylene blue onto sepiolite, Dyes Pigm., 75 (2007) 701–713.

[11] A. Rodríguez, G. Ovejero, M. Mestanza and J. García, Removal of dyes from wastewaters by adsorption on sepiolite and pansil, Ind. Eng. Chem. Res., 49 (2010) 3207–3216.
[12] A. Rodríguez, J. García, G. Ovejero and M. Mestanza, Adsorption of anionic and cationic dyes on activated carbon from aqueous solutions: Equilibrium and kinetics, J. Hazard. Mater., 173 (2009) 1311–1320.
[13] G. Atun, G. Hisarlin, W.S. Sheldrick and M. Muhler, Adsorptive removal of methylene blue from colored effluents on fuller's earth, J. Colloid Interface Sci., 261 (2003) 32–39.
[14] C.H. Giles, T.H. MacEwan, S.N. Nakhwa and D. Smith, Studies in adsorption, Part XI: A system of classification of solution adsorption isotherms, and it use in diagnosis of adsorption mechanisms and in measurement of specific surface area of solids, J. Chem. Soc., 111 (1960) 3973–3993.
[15] A. Rodríguez, J. García, J.L. Sotelo, G. Ovejero and M. Mestanza, Removal of the pesticides diuron and carbofuran in aqueous solutions by activated carbon, Fresen. Environ. Bull., 18 (2009) 2093–2101.
[16] C.H. Wu, Adsorption of reactive dye onto carbon nanotubes: Equilibrium, kinetics and thermodynamics, J. Hazard. Mater., 144 (2007) 93–100.
[17] D.D. Do, Adsorption analysis: Equilibria and kinetics, Imperial College Press, London, 1998, pp. 48–148.
[18] H. Babaki, A. Salem and A. Jafarizad, Kinetic model for the isothermal activation of bentonite by sulfuric acid, Mater. Chem. Phys., 108 (2008) 263–268.
[19] G. Hisarli, The effects of acid and alkali modification on the adsorption performance of fuller's earth for basic dye, J. Colloid Interface Sci., 281 (2005) 18–26.
[20] D. Ghosh and K.G. Bhattacharyya, Adsorption of methylene blue on kaolinite, Appl. Clay Sci., 20 (2002) 295–300.
[21] N. Schouten, L.G.J. van der Ham, G.J.W. Euverink and A.B. de Haan, Selection and evaluation of adsorbents for the removal of anionic surfactants from laundry rinsing water, Water Res., 41 (2007) 4233–4241.
[22] A. Tabak, B. Afsin, B. Caglar and E. Koksal, Characterization and pillaring of a Turkish bentonite (Resadiye), J. Colloid Interface Sci., 313 (2007) 5–11.
[23] N.J. Saikia, D.J. Bharali, P. Sengupta, D. Bordoli, R.L. Goswamee, P.C. Saikia and P.C. Borthakur, Characterization, beneficiation and utilization of a kaolinite clay from Assam, India, Appl. Clay Sci., 24 (2003) 93–103.
[24] M.A. Qtaitat and I.N. Al-Traqneh, Characterization of kaolinite of the Baten El-Ghoul region/south Jordan by infrared spectroscopy, Spectrochim. Acta, Part A, 61 (2005) 1519–1523.
[25] M. Suárez and E. García–Romero, FTIR spectrosocpic study of paligoskite: Influence of the composition of the octahedral sheet, Appl. Clay Sci., 31 (2006) 154–163.
[26] J. Temuujin, Ts. Jadambaa, G. Bruma, Sh. Erdenechimeg, J. Amarsanaa and K.J.D. MaxKenzie, Characterization of acid activated montmorillonite clay from Tuulant (Mongolia), Ceram. Int., 30 (2004) 251–255.
[27] T.S. Anirudhan and P.S. Suchithra, Synthesis and characterization of tannin-immobilized hydrotalcite as a potential adsorbent of heavy metal ions in effluent treatments, Appl. Clay Sci., 42 (2008) 214–233.
[28] Y.L. Ma, Z.R. Xu, T. Guo and P. You, Adsorption of methylene blue on Cu(II)-exchanged montmorillonite, J. Colloid Interface Sci., 280 (2004) 283–288.
[29] M.Y. Chang and R.S. Juang, Adsorption of tannic acid, humic acid, and dyes from water using the composite of chitosan and activated clay, J. Colloid Interface Sci., 278 (2004) 18–25.
[30] Z. A-Qodah, W.K. Lafi, Z. Al-Anber, M. Al-Shannag and A. Harahsheh, Adsorption of methylene blue by acid and heat treated diatomaceous silica, Desalination, 217 (2007) 212–24.
[31] A. Gürses, Ç. Doğar, M. Yalçın, M. Açıkyıldız, R. Bayrak and S. Karaca, The adsorption kinetics of the cationic dye, methylene blue, onto clay, J. Hazard. Mater., 131 (2006) 217–228.
[32] S. Wang, H. Li and L. Xu, Application of zeolite MCM-22 for basic dye removal from wastewater, J. Colloid Interface Sci., 295 (2006) 71–78.
[33] A. Rodríguez, G. Ovejero, M. Mestanza and J. García, Adsorption of dyes on carbon nanomaterials from aqueous solutions, J. Environ. Sci. Health., Part A, 45 (2010) 1642–1653.
[34] L. Abramian and H. El-Rassy, Adsorption kinetics and thermodynamics of azo-dye Orange II onto highly porous titania aerogel, Chem. Eng. J., 150 (2009) 403–410.
[35] C. Hsiu-Mei, C. Ting-Chien, P. San-De and C. Hung-Lung, Adsorption characteristics of Orange II and Chrysophenine on sludge adsorbent and activated carbon fibers, J. Hazard. Mater., 161 (2009) 1384–1390.